MAT JOURNALS
Journal of Mechanical and Mechanics Engineering
Volume 3 Issue 1

Effect of Pulsed Current Micro Plasma Arc parameters on weld bead geometry of AISI 316Ti Austenitic Stainless Steel

Kondapalli Siva Prasad[1], Tarun Bayya[2]
[1]Associate Professor, Dept. of Mechanical Engineering, Anil Neerukonda Institute of Technology & Sciences,Visakhapatnam, India
Email: kspanits@gmail.com, Contact No: +91-9849212391
[2] UG student, Dept. of Mechanical Engineering, Anil Neerukonda Institute of Technology & Sciences,Visakhapatnam, India
Email: sonukick55@gmail.com, Contact No: +91-9032528727

Abstract
Micro Plasma Arc Welding (MPAW) is one of the important arc welding system normally using in sheet metal enterprise for production metal bellows, metallic diaphragms and so forth. Inside the present work Pulsed present day Micro Plasma Arc Welding is used for becoming a member of 0.three mm thick Austenitic stainless-steel sheets of AISI 316 Ti. peak contemporary, Base modern, Pulse rate and Pulse Width are taken into consideration as input parameters and weld bead geometry parameters namely front width, lower back width, front peak, lower back peak are taken into consideration as output responses. Response surface approach (RSM) with box-Benhken design is adopted and for 4 factors and three level, total 27 experiments are completed. Weld bead geometry parameters particularly front width, returned width, the front height and lower back top are measured the use of metallurgical microscope. Empirical mathematical models are evolved using statistical software. Analysis of Variance (ANOVA) is executed at ninety five% self belief degree. Predominant and interplay outcomes are studied. Scatter plots are attracted to apprehend the version of actual and predicted values of weld bead parameters.

Keywords:*Plasma Arc Welding, Austenitic Stainless Steel, Weld bead geometry, AISI 316Ti*

INTRODUCTION

In 1964 plasma arc welding process was introduced to the welding industry as a method of bringing better control to the arc welding process in lower current ranges [1].It is used to produce high quality welds in both miniature and pre precision applications and to provide long electrode life for high production requirements at all levels of amperage. Plasma welding is equally suited to manual and automatic applications. It is used in a variety of joining operations ranging from welding of miniature components to seam welding, to high volume production welding, and many others.

From the literature it is understood that N.M.Voropai et.al [2] developed a technique of pulsed micro plasma butt welding for welding shells of asbestos-metal gaskets made of Aluminium of thickness 0.2-0.3mm. Pulsed micro plasma welding results in steady burning of the arc on low current and in the destruction of the oxide film on the joined metal. In this method, argon of a purity of not less than 99.8% is used as plasma forming gas and helium of a purity of not less than 99.5% as protective gas. A.S.Sepokurov et.al [3] developed a device for controlling welding current , so that it can be used for welding thin components and for hard facing small components. W.Luo et.al [4] analysed the floor microstructure and the anodic

polarization curves in a 1 N H2SO4 answer of a 0Cr19Ni9 metal submerged arc welded joint earlier than and after surface melting using a four-A micro-plasma arc. The results showed that both the heat-affected sector and the weld metal of the as-welded joint had a lower corrosion resistance than the as-acquired discern material, at the same time as the arc melted joint had a significantly expanded corrosion resistance. This growth in corrosion resistance is attributed to a speedy solidification of the melted layer. Rapid solidification of the melted layer refines its microstructure, decreases micro segregation and inhibits the precipitation of chromium carbides at the grain obstacles. F. Karimzadeh et.al [5] investigated the effect of micro plasma arc welding (MPAW) process parameters on grain growth and porosity distribution of thin sheet Ti6Al4V alloy weldment. The MPAW process was completed at exclusive current, welding pace and flow fees of protecting & plasma fuel. square-butt welding in a unmarried bypass, the usage of direct contemporary and instantly polarity (DCEN) became selected for the welding technique. The titanium alloy studied in the present experiment is a thin sheet of Ti6Al4V alloy with a thickness of 0.8mm.F. Karimzadeh et.al [6] examined the effect of epitaxial growth on microstructure of Ti–6Al–4V alloy weldment by artificial neural networks (ANNs). The micro plasma arc welding (MPAW) procedure was performed at different currents, welding speeds and flow rates of shielding & plasma gas. Micro structural characterizations were studied by optical and scanning electron microscopy (SEM). Finally, an artificial neural network was developed to predict grain size of fusion zone (FZ) at different currents and welding speeds. Pei-quanXu et.al [7] evolved a model to simulate the electromagnetic phenomena and fluid discipline in plasma arc occurring throughout the low-cutting-edge micro plasma arc welding manner. Mentioned the results of the nozzle neck-in and welding modern-day of micro-plasma arc at the arc electromagnetic discipline distribution.

From the works said on plasma arc welding, it is understood that maximum of the works mentioned on better thickness, very few works are suggested on thickness less than 0.3mm. So, it is intended to have a look at the impact of pulsed MPAW method parameters on weld bead geometry parameters of zero.3 mm thick Austenitic chrome steel sheets of AISI 316 Ti, which might be used for steel bellow manufacturing. peak current, Base modern-day, Pulse charge and Pulse Width are considered as input parameters and weld bead geometry parameters specifically the front width, returned width, the front peak, returned height are considered as output responses.

EXPERIMENTAL PROCEDURE

Weld specimens of 100 x 150 x 0.3mm size are prepared from AISI 316Ti sheets and joined using square butt joint. The chemical composition and tensile properties of AISI 316Ti stainless steel sheet as provided by M/s Metallic Bellows (I) Pvt Ltd, Chennai, India are presented in Table .1 & 2. Argon is used as a shielding gas and a trailing gas to avoid contamination from outside atmosphere. The welding conditions adopted during welding are presented in Table .3. From the earlier works [8-11] carried out on Pulsed Current MPAW it was understood that the peak current, back current, pulse rate and pulse width are the dominating parameters which effect the weld quality characteristics. The values of process parameters used in this study are the optimal values obtained from our earlier papers [8-11]. Hence peak current, back current, pulse rate and pulse width are chosen as parameters and their levels are

presented in Table .4. Details about experimental setup are shown in Figure.1

Fig .1 *Micro Plasma Arc Welding Setup.*

Table .1 Chemical composition of AISI 316Ti (weight %)

C	Si	Mn	P	S	Cr	Ni	N
0.05	0.52	1.30	0.028	0.021	17.48	9.510	0.04

Table .2 Mechanical properties of AISI 316Ti

Elongation (%)	Yield Strength (MPa)	Ultimate Tensile Strength (Mpa)
53.20	272.15	656.30

Table .3 Welding conditions

Power source	Secheron Micro Plasma Arc Machine (Model: PLASMAFIX 50E)
Polarity	DCEN
Mode of operation	Pulse mode
Electrode	2% thoriated tungsten electrode
Electrode Diameter	1mm
Plasma gas	Argon & Hydrogen
Plasma gas flow rate	6 Lpm
Shielding gas	Argon
Shielding gas flow rate	0.4 Lpm
Purging gas	Argon
Purging gas flow rate	0.4 Lpm
Copper Nozzle diameter	1mm
Nozzle to plate distance	1mm
Welding speed	260mm/min
Torch Position	Vertical
Operation type	Automatic

Table .4 *Process parameters and their limits.*

		Levels		
Input Factor	Units	-1	0	+1
Peak Current	Amps	6	7	8
Base Current	Amps	3	4	5
Pulse rate	Pulses /Sec	20	40	60
Pulse width	%	30	50	70

Three metallurgical samples are cut from every joint leaving the rims of faulty part of the welded period. Defective period of weld is recognized visually and also by way of conducting dye pentrant and X-ray exams and installed using Bakelite. pattern instruction and mounting is carried out as in line with ASTM E 3-1 standard. The transverse face of the samples are floor the use of one hundred twenty grit length belt with the assist of belt grinder and polished sequentially the use of grade 1/zero (245 mesh length), grade 2/0(425 mesh length) and grade 3/0 (515 mesh size) sand paper. The specimens are further polished using aluminium oxide, diamond paste and velvet cloth on a disc polishing machine. The polished specimens are macro-etched using 10% Oxalic acid solution to reveal the geometry of the weld bead. Several critical parameters, such as front width, back width, front height and back height of the weld bead geometry are measured using Metallurgical Microscope (Make: De winter Technologies, Model No. DMI-CROWN-II) at 100X magnification. Figures.3indicates the macrographs of front width, back width, front height and back height. The measured dimensions of weld bead geometry parameters are presented in Table 5. The typical weld bead geometry is shown in Figure.2.

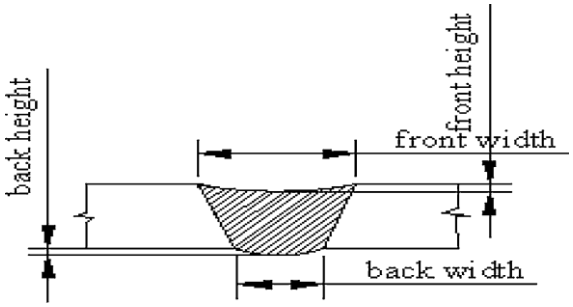

Fig.2*Typical weld bead geometry*

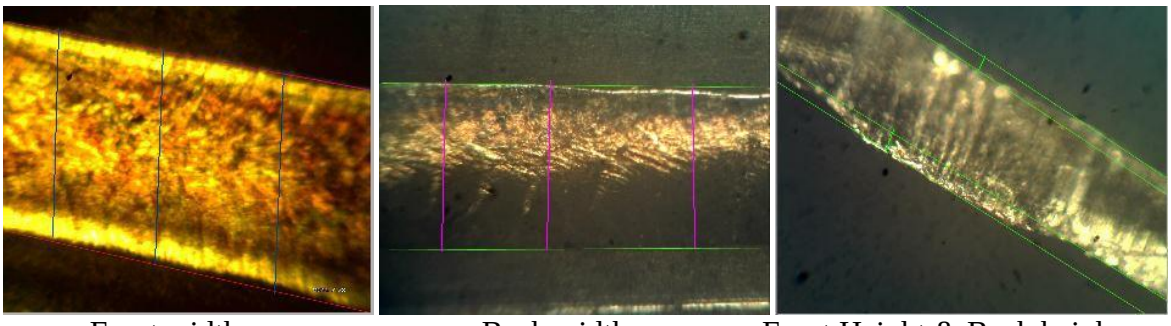

Front width Back width Front Height & Back heigh

Fig.3*Metallographic images of weld bead*

Evaluation OF EXPERIEMNTAL data

The experiments had been conducted as in line with the design matrix (table.5) and the values of weld bead geometry measured by way of metallurgical microscopes are supplied.

Table .5 *Experimental Results*

Exp No.	Peak Current (Amps)	Base current (Amps)	Pulse Rate (Pulses/ sec)	Pulse width (%)	Front Width (mm)	Back Width (mm)	Front Height (mm)	Back Height (mm)
1	6	3	40	50	0.741	0.563	0.160	0.096
2	8	3	40	50	0.720	0.547	0.156	0.092
3	6	5	40	50	0.781	0.594	0.154	0.091
4	8	5	40	50	0.840	0.640	0.110	0.064
5	7	4	20	30	0.674	0.511	0.162	0.096
6	7	4	60	30	0.977	0.747	0.134	0.078
7	7	4	20	70	0.792	0.603	0.174	0.103
8	7	4	60	70	0.733	0.557	0.172	0.102
9	6	4	20	50	0.821	0.625	0.152	0.089
10	8	4	60	50	0.962	0.735	0.116	0.067
11	6	4	20	50	0.821	0.625	0.152	0.089
12	8	4	20	50	0.730	0.555	0.153	0.090
13	7	3	60	30	0.846	0.645	0.135	0.079
14	7	5	40	30	0.797	0.607	0.128	0.074
15	7	3	40	50	0.733	0.557	0.166	0.098
16	7	5	40	50	0.813	0.619	0.145	0.085
17	6	4	40	30	0.807	0.614	0.144	0.084
18	8	4	40	30	0.804	0.612	0.135	0.079
19	6	4	40	70	0.722	0.548	0.181	0.107
20	8	4	40	70	0.762	0.580	0.149	0.087
21	7	3	20	50	0.734	0.558	0.181	0.107
22	7	5	20	50	0.725	0.550	0.138	0.080
23	7	3	60	50	0.765	0.581	0.152	0.089
24	7	5	60	50	0.912	0.696	0.158	0.093
25	7	4	40	50	0.836	0.637	0.171	0.101
26	7	4	40	50	0.815	0.621	0.169	0.100
27	7	4	40	50	0.846	0.645	0.167	0.099

Development of mathematical models

Using MINITAB 14 statistical software package, the significant coefficients were determined and final model is developed using coefficients to estimate the Front width, Back width, Front Height and Back Height of weld joint.

Front width = $0.486608 - 0.113118X_1+0.262821X_2-0.015534X_3 - 0.006870X_4 - 0.055780X_2^2 +0.000026X_3^2 -0.000121X_4^2 +0.020X_1X_2 +0.002811X_1X_3+0.0005387X_1X_4 +0.001926X_2X_3 -0.000227X_3X_4$

Back width = $0.356779 - 0.085568X_1+0.204859X_2-0.011758X_3 +0.12022X_4 - 0.043488X_2^2 -0.000020X_3^2 - 0.000094X_4^2 +0.015500X_1X_2 +0.002811X_1X_3 +0.00042587X_1X_4 +0.001515X_2X_3 -0.000177X_3X_4$

Front Height = $-0.974513 +0.275176X_1 +0.081475X_2+0.002054X_3 +0.001089X_4 - 0.0014704X_1^2-0.007914X_2^2 -0.000004X_4^2 -0.010000 X_1X_2-0.000667X_1X_3- 0.000288X_1X_4 +0.0.000611X_2X_3 +0.000016X_3X_4$

Back Height = $-0.586478+0.167319X_1 +0.044933X_2+0.001339X_3 +0.000643X_4 - 0.008947X_1^2-0.004806X_2^2 -0.000007X_4^2 - 0.005750X_1X_2-0.000425X_1X_3-$

$0.000188X_1X_4$ $+0.000387X_2X_3$ $+0.000011X_3X_4$

where X_1,X_2, X_3 , X_4 are the coded values of peak current, base current, pulse rate and pulse width.

Checking the adequacy of the developed model

The adequacy of the developed models is tested for 95% confidence using Analysis of Variance (ANOVA) and presented in Table.6. Figure .4 to 7 indicate the scatter plot Front width, Back width, Front Height and Back Height of weld joint and reveals that the experimental and predicted values are close to each other within the specified limits.

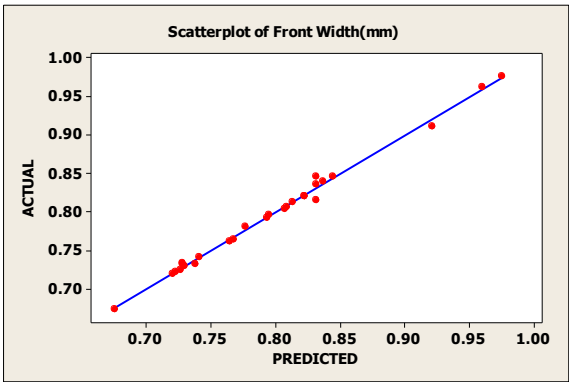

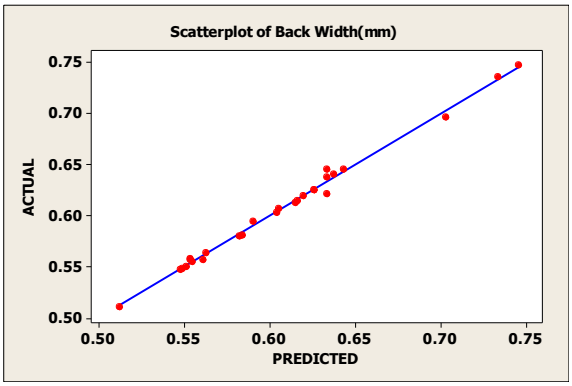

Fig.4*Scatter plot for Front Width* ***Fig .5****Scatter plot for Back Width*

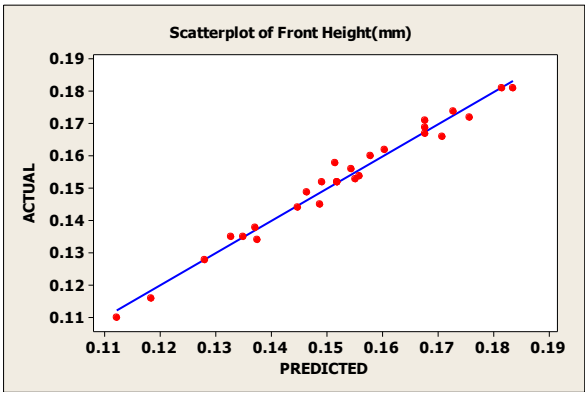

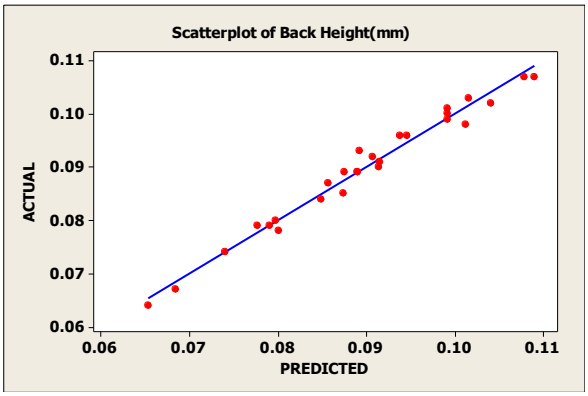

Fig .6*Scatter plot for Front Width* ***Fig .7****Scatter plot for Back Height*

Table 6 Analysis of Variance

Analysis of Variance for Front Width(mm)						
Source	DF	Seq SS	Adj SS	Adj MS	F	P
Regression	14	0.136332	0.136332	0.009738	155.69	0.000
Linear	4	0.055549	0.012725	0.003181	50.86	0.000
Square	4	0.029189	0.016983	0.004246	67.88	0.000
Interaction	6	0.051594	0.051594	0.008599	137.48	0.000
Residual Error	12	0.000751	0.000751	0.000063		
Lack-of-Fit	9	0.000250	0.000250	0.000028	0.17	0.984
Pure Error	3	0.000501	0.000501	0.000167		
Total	26	0.137082				
Analysis of Variance for Back Width(mm)						
Source	DF	Seq SS	Adj SS	Adj MS	F	P
Regression	14	0.082548	0.082548	0.005896	152.91	0.000
Linear	4	0.033567	0.007661	0.001915	49.67	0.000
Square	4	0.017610	0.010279	0.002570	66.64	0.000
Interaction	6	0.031371	0.031371	0.005228	135.59	0.000
Residual Error	12	0.000463	0.000463	0.000039		
Lack-of-Fit	9	0.000164	0.000164	0.000018	0.18	0.980
Pure Error	3	0.000299	0.000299	0.000100		
Total	26	0.083010				
Analysis of Variance for Front Height(mm)						
Source	DF	Seq SS	Adj SS	Adj MS	F	P
Regression	14	0.008534	0.008534	0.000610	41.49	0.000
Linear	4	0.004842	0.001881	0.000470	32.00	0.000
Square	4	0.001756	0.001255	0.000314	21.36	0.000
Interaction	6	0.001935	0.001935	0.000323	21.95	0.000
Residual Error	12	0.000176	0.000176	0.000015		
Lack-of-Fit	9	0.000168	0.000168	0.000019	7.01	0.068
Pure Error	3	0.000008	0.000008	0.000003		
Total	26	0.008710				
Analysis of Variance for Back Height(mm)						
Source	DF	Seq SS	Adj SS	Adj MS	F	P
Regression	14	0.003288	0.003288	0.000235	39.68	0.000
Linear	4	0.001869	0.000700	0.000175	29.57	0.000
Square	4	0.000658	0.000460	0.000115	19.45	0.000
Interaction	6	0.000760	0.000760	0.000127	21.40	0.000
Residual Error	12	0.000071	0.000071	0.000006		
Lack-of-Fit	9	0.000069	0.000069	0.000008	11.50	0.035
Pure Error	3	0.000002	0.000002	0.000001		
Total	26	0.003359				

Effect of welding parameters

Graphs are drawn for each welding parameters separately (Figure.8 to 11) and the following observations are made:

Front Width and Back width increases with increase in peak current, base current and pulse rate, where as it decreases with increase in pulse width. This is because , as the current increases heat input

increases, which leads to more melting of base metal and hence wider width on front side of the weld bead. Pulse width has negative effect on heat input, larger the pulse width lesser the heating time, which leads to low melting of base metal and lower width on front side of the weld bead. Front Height and Back Height decreases with increase in peak current, base current and pulse rate, where as it increases with increase in pulse width. This is because, as the current increases heat input increases, which leads to more melting of base metal. Because of higher melting rate, the weld bead is wider, but it has less narrow depth (front height and back height).Pulse width has negative effect on heat input, larger the pulse width lesser the heating time, which leads to low melting of base metal. Because of lower melting rate, the weld bead is narrow width, but it has higher narrow depth (front height and back height).

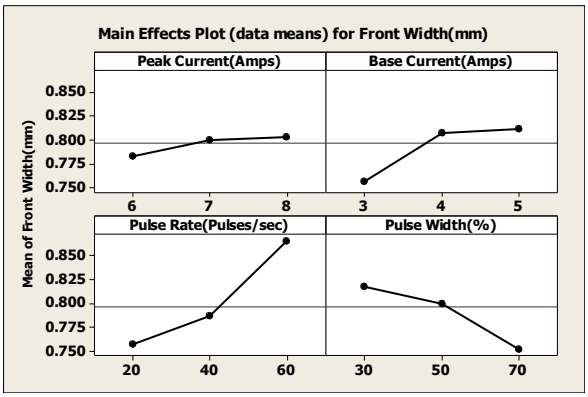

Fig .8*Main effect on Front Width*

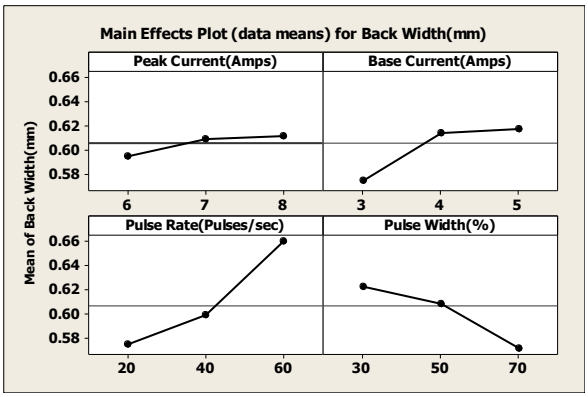

Fig .9*Main effect on Back width*

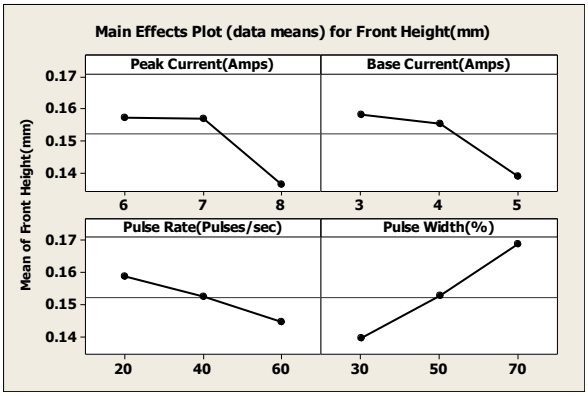

Fig .10*Main Effect on Front Height*

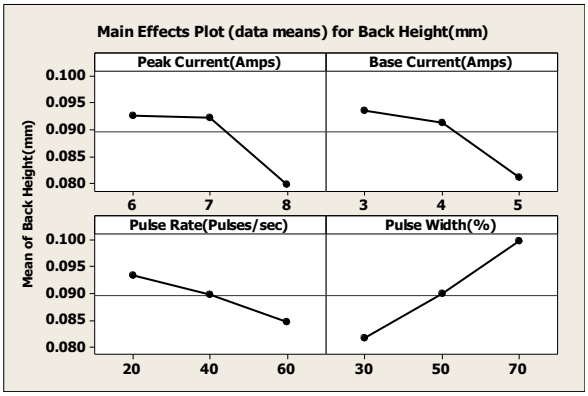

Fig .11 *Main effect for Back Height*

CONCLUSIONS

From the experiments performed and developed models the following results are drawn.

a. The developed empirical mathematical models are used for predicted the weld bead geometry parameters for the given input parameters within the range of selected input parameters.
b. From the scatter plot it is understood that experimental and predicted values are close to each other.
c. Front width and Back width increases with increase in peak current, back current and pulse rate .However they decrease with increase in pulse width. The higher front width and Back width is due to more heat input because of higher currents. Front height and Back

height decreases with increase in peak current, back current and pulse rate. However they increase with increase in pulse width.

d. Peak current is the most dominating factor effecting weld bead geometry followed by base current, pulse rate and pulse width.
e. Optimal weld bead geometry is obtained at a peak current is 7 Amps, Base current is 4 Amps, Pulse rate of 60 pulses/sec and pulse width of 30%.
e. The developed mathematical models for weld bead geometry parameters are valid only for 0.3mm thick AISI 316Ti Austenitic Stainless Steel
f. The developed model is valid within the specified range of the selected welding parameters; however the accuracy can be improved by considering more number of factors and their levels.

REFERENCES

1. Jean Marie Fortain, Plasma welding evolution & challenges, Air Liquide CTAS, Welding and Cutting Research Center, 95315 CergyPontoise France, 2010;p.11.

2. N.M.Voropai, V.V.Shcherbak and A.A.Grigorev, Pulsed Microplasma welding of thin Aluminum gaskets, Equipment Manufacturing Technology,1971,11, p.19.

3. A. S.Sepokurov, G.I.Sergatskii and A.P.Alikin, , Use of Microplasma welding in component construction, Japan welding society, 1971; 11, p.20.

4. W. Luo, Effect of micro-plasma arc melting on the corrosion resistance of a 0Cr19Ni9 stainless steel SAW joint, Materials Letters , 55,2002,pp. 290–295.

5. Karimzadeh, F. , Salehi, M. , Saatchi, A. and Meratian, M, Effect of micro plasma arc welding process parameters on grain growth and porosity distribution of thin sheet Ti6Al4V alloy weldment, Materials and Manufacturing Processes, 2005; 20(2), pp.205 - 219.

6. F. Karimzadeh , A. Ebnonnasir , A. Foroughi , Artificial neural network modeling for evaluating of epitaxial growth of Ti6Al4V weldment, Materials Science and Engineering , 2006;A 432 ,pp.184–190.

7. Pei-quanXu , Shun Yao, Jian-ping He, Chun-wei Ma & Jiang-weiRen, Numerical analysis for effect of process parameters of low-current micro-PAW on constricted arc, Int J AdvManufTechnol , 2009; 44, pp.255–264.

8. Kondapalli Siva Prasad, Ch.SrinivasaRao, D.NageswaraRao, Application of Grey Relational Analysis for Optimizing Weld pool geometry parameters of Pulsed Current Micro Plasma Arc Welded Inconel 625 sheets, International Journal of Advanced Manufacturing Technology (Springer), 2015, DOI 10.1007/s00170-014-6665-y .

9. K. Siva Prasad, Ch.SrinivasaRao, D.NageswaraRao, (2012),Effect of process parameters of pulsed current micro plasma arc welding on weld pool geometry of Inconel 625 welds, Kovove Materialy - Metallic Materials, 2012;0(3),pp.153-159.

10. Kondapalli Siva Prasad, Ch.Srinivasa Rao, D. Nageswara Rao, Application of Grey Relational Analysis for Optimizing Weld pool geometry parameters of Pulsed Current Micro Plasma Arc Welded AISI 304L

stainless steel sheets, International Journal of Advanced Design and Manufacturing Technology , 2013; 6(1),79-86p.
11. Kondapalli Siva Prasad, Ch.Srinivasa Rao,D.NageswaraRao, Multi-objective Optimization of Weld Bead Geometry Parameters of Pulsed Current Micro Plasma Arc Welded AISI 304L Stainless Steel Sheets Using Enhanced Non-dominated Sorting Genetic Algorithm, Journal of Manufacturing science and production, 2014;14(2),pp.79-85.